Copper Chaperone Atox1 Interacts with Cell Cycle Proteins

Computational and Structural Biotechnology Journal 16 (2018) 443–449

COMPUTATIONAL AND STRUCTURAL BIOTECHNOLOGY JOURNAL

journal homepage: www.elsevier.com/locate/csbj

Copper Chaperone Atox1 Interacts with Cell Cycle Proteins

Maria Matson Dzebo, Stéphanie Blockhuys, Sebastian Valenzuela, Emanuele Celauro, Elin K. Esbjörner, Pernilla Wittung-Stafshede *

Department of Biology and Biological Engineering, Chalmers University of Technology, 412 96 Gothenburg, Sweden

ARTICLE INFO

Article history:
Received 13 September 2018
Received in revised form 20 October 2018
Accepted 26 October 2018
Available online 31 October 2018

ABSTRACT

The anaphase-promoting complex (APC) is involved in several processes in the cell cycle, most prominently it facilitates the separation of the sister chromatids during mitosis, before cell division. Because of the key role in the cell cycle, APC is suggested as a putative target for anticancer agents. We here show that the copper chaperone Atox1, known for shuttling copper in the cytoplasm from Ctr1 to ATP7A/B in the secretory pathway, interacts with several APC subunits. Atox1 interactions with APC subunits were discovered by mass spectrometry of co-immunoprecipitated samples and further confirmed using proximity ligation assays in HEK293T cells. Upon comparing wild-type cells with those in which the Atox1 gene had been knocked out, we found that in the absence of Atox1 protein, cells have prolonged G_2/M phases and a slower proliferation rate. Thus, in addition to copper transport for loading of copper-dependent enzymes, Atox1 may modulate the cell cycle by interacting with APC subunits.

1. Introduction

Copper (Cu) ions in oxidized and reduced forms are found in the active sites of many essential proteins that participate in key cellular reactions often involving electron transfer [1–3]. However, free Cu ions are potentially toxic for cells since, due to their redox activity, they are capable of producing reactive oxygen species [4]. To avoid Cu toxicity, the intracellular concentration of Cu is regulated via dedicated proteins that facilitate uptake, efflux as well as distribution of Cu to Cu-dependent proteins and enzymes [5–7]. In the human cytoplasm, after the uptake of Cu ions by the membrane-spanning Ctr1 trimer [8], the small Cu chaperone Atox1 transports the metal to ATP7A and ATP7B (also called Menke's and Wilson disease proteins, respectively), two homologous membrane-bound P_{1B}-type ATPases located in the trans-Golgi network. Once transferred to ATP7A/B, the Cu ion is channeled to the lumen of the Golgi where it is loaded onto Cu-dependent proteins and enzymes in the secretory pathway [9–12].

However, it is becoming more and more obvious that the concept of 'one protein – one function' is naive. Many proteins appear to have multiple functions and this has become clear also for Atox1. In 2008, Atox1 was reported to have additional activity in the nucleus as a Cu-dependent transcription factor (TF) of several genes [13–17]. We also confirmed the presence of Atox1 in the nucleus of HeLa cells, but no DNA binding of Atox1 to the proposed GAAAGA promotor sequence *in vitro* was detected [18]. Nonetheless, Atox1 may regulate gene transcription via additional proteins that in turn bind DNA. Using a yeast two-hybrid screen of a large human fragment library, a number of new Atox1-interacting proteins were identified as confident hits [19]. Among these target proteins, several were reported as detected in the nucleus and described as DNA/RNA-binding proteins [19]. However, these experiments were made in yeast and may not necessarily represent interactions taking place in human cells. In addition, Atox1 was found to localize at lamellipodia edges in breast cancer cells and, by a yet unknown mechanism, promote cancer cell migration [20]. Clearly, Atox1 may have more activities than basic copper transport to the secretory pathway [9,21].

To reveal Atox1 interaction partners in human cells, we here developed a co-immunoprecipitation protocol for Atox1 in human embryonic kidney (HEK293T) cells and used it, together with mass spectrometry analysis, to identify new protein interactions. The results revealed that several Atox1 interaction partners are subunits of the large multiprotein anaphase-promoting complex (here abbreviated as APC; also called cyclosome, or APC/C). APC is a cullin-RING E3 ubiquitin ligase that facilitates chromatid separation in mitosis before cell division, but it also has additional cell cycle functions such regulation of cyclins [22,23]. We direct readers to several excellent reviews for information on function and mechanism of APC [22,24–26]. Therefore, after

* Corresponding author.
E-mail address: Pernilla.wittung@chalmers.se (P. Wittung-Stafshede).

https://doi.org/10.1016/j.csbj.2018.10.018

confirming some Atox1-APC interactions in cells using the *in situ* proximity ligation assay, we used Atox1 knock-out (KO) cells to investigate the putative role of Atox1 in the cell cycle and proliferation of HEK293T cells.

2. Materials and Methods

2.1. Cell Culture

HEK293T and MDA-MB-231 cells were purchased from ATCC (Manassas, VA, USA). The cells were cultured in Dulbecco's modified Eagle's medium containing high glucose, pyruvate and L-glutamine (Gibco), supplemented with 10% fetal bovine serum (Hyclone, GE healthcare), at 37 °C in a humidified atmosphere with 5% CO_2. Cells were washed with DPBS without calcium and magnesium (Gibco) once and detached using TrypLE express (Gibco) at a confluency of about 80% for subculturing.

2.2. Atox1 KO Cell Line

We used CRISPR-Cas9 technology coupled to LoxP-driven recombination to establish an Atox1 KO cell line of HEK293T cells. Unlike in standard knock-out strategies, where the reading frame and the transcription start site are simply disrupted by the insertion of a reporter/selection cassette, we opted for a complete excision of the *Atox1* genomic locus, by knocking in two LoxP sites, flanking the locus itself. To obtain this, after synchronization for 16 h with 10 mM Ro-3306 CDK1 inhibitor (Sigma Aldrich), HEK293T cells were washed with DPBS without calcium and magnesium (Gibco), detached with Tryple Express (ThermoFisher) washed again in DPBS and re-suspended in the electroporation mix, containing the pre-assembled Cas9(v2)/gRNA ribonucleoprotein (Life Technologies) and the ssDNA template for each LoxP cassette (Eurofins Genomics).

Cells were immediately electroporated using a Neon Transfection System (ThermoFisher) (pulse voltage 1150 V, pulse width 20 ms, 2 pulses) and a 10 μL tip. The electroporated cells were expanded and genomic DNA extracted from an aliquot to verify the correct insertion of each LoxP cassette, flanking the *Atox1* locus. Once confirmed both LoxP cassettes, the addition of Cre recombinase-containing gesicles (Clontech, Takara) directly to the culture medium allowed the 'floxing out', i.e. the excision, of the entire *Atox1* locus through recognition of the two oriented LoxP sites. At this stage, the floxed culture was still a mix of edited and non-edited cells (Fig. S1) and clonal isolation by serial dilution was performed. Different monoclonal lines were expanded and lack of Atox1 in each was analyzed by immunostainings and Western blots. Only one of the cell lines showing a complete lack of Atox1, further verified by PCR, was then used for the experiments involving KO cells. The KO cells were cultured under the same conditions as wild-type (wt) cells.

Identification of Cas9 target sequences for the insertion of the LoxP cassettes was made with the Dharmacon online tool (http://dharmacon.gelifesciences.com/gene-editing/crispr-cas9/crispr-design-tool/). The design of the two sgRNA(−L/R) and the resulting ssDNA templates, to exploit the homology-directed repair pathway to introduce the LoxP cassettes, was performed with the Dharmacon web tool (http://dharmacon.horizondiscovery.com/gene-editing/crispr-cas9/edit-r-hdr-donor-designer-oligo/). Sequences used (5′-3′):

sgRNA-L: ACCACTCACCGGCATGACTG (<)

sgRNA-R: ATGGACCAAAGGGGGCAGGT (>)

LoxP: ATAACTTCGTATAATGTATGCTATACGAAGTTAT (<) - 34 bp

Atox1.LoxP-L ssDNA: GGC GCT GCT GAC ACC GCC GCC ACA CCG CCG CCA CAC CGC CGC TGC CTC AGA TAA CTT CGT ATA GCA TAC ATT ATA CGA AGT TAT TCA TGC CGG TGA GTG GTT GCG CCG TCC CCG CCA CGC AGA CTT GCA GTC CC

Atox1.LoxP-R ssDNA: AGT AGC AGG GGC CTG GTC CCC ACA GCC CAC AGG ATG GAC CAA AGG GGG CAA TAA CTT CGT ATA GCA TAC ATT ATA CGA AGT TAT GGT GGG TAA GGC CCC AGC ACT TGC TGA ACA AAC CTA CAG CTC ACA CCT CT.

2.3. Lysis of Cells

Cells (80% confluency) were washed with DPBS prior to lysing with lysis buffer (Pierce IP lysis buffer, Thermo Scientific) and incubated at 4 °C for 10 min on a rotary shaker. The lysate was centrifuged at 13,000*g* for 10 min at 4 °C and the supernatant was used for further studies.

2.4. Co-Immunoprecipitation (Co-IP)

Co-IP was performed with Pierce MS-compatible Magnetic IP Kit (ThermoFisher) using an adapted protocol. Magnetic beads (50 uL) were washed 3 times with coupling buffer. 10 μg rabbit anti-Atox1 monoclonal antibody (Abcam) or 10 μg rabbit monoclonal IgG isotype control antibody (Abcam) in 500 uL coupling buffer (20 mM Na phosphate pH 7–9, 150 mM NaCl, 0.05% Tween 20) was added to the washed beads and the solution was incubated for 15 min at room temperature (vortexed every 5 min). The antibody-conjugated beads were washed with coupling buffer three times before incubation with 5 mM disuccinimidyl suberate (DSS, ThermoFisher) during 45 min at room temperature on a tube rotator. To quench crosslinking, TRIS buffer (prepared from Trizma-HCl, Sigma Aldrich) was added to a final concentration of 25 mM and the beads were incubated on the tube rotator 15 min at room temperature prior to three washes with coupling buffer. The beads were further blocked with 1× Roti-Block (Carl Roth) for 30 min at 4 °C with rotation and then mixed with pre-cleared cell lysate (cell lysate incubated 30 min at 4 °C with magnetic beads, without antibodies, to avoid non-specific binding to the beads). The beads were incubated with the pre-cleared cell lysate during 4 h and then washed with the wash buffers in the kit according to the manufacturer's recommendation (5 washes in total). Elution was done with 100 μL elution buffer during 10 min. Upon Western blot detection of Atox1, the samples were sent for analysis the Proteomics Core Facility at the Sahlgrenska Academy, University of Gothenburg.

Eluates from the IP were digested with trypsin using modified filter-aided sample preparation (FASP) protocol [27]. Briefly, sodium dodecyl sulfate (SDS) and triethylammonium bicarbonate (TEAB) were added to final concentrations of 2% SDS and 50 mM TEAB prior to reduction using 100 mM dithiothreitol at 60 °C for 30 min. Reduced samples were transferred and concentrated onto 10 kDa MWCO Pall Nanosep centrifugal filters (Sigma-Aldrich) and washed repeatedly with 8 M Urea. Alkylation was performed with 10 mM methyl methane thiosulfonate (MMTS) diluted in digestion buffer (1% sodium deoxycholate (SDC), 50 mM TEAB) for 30 min in room temperature. Trypsin (0.3 μg, Pierce Trypsin Protease, MS Grade, Thermo Fisher Scientific) in digestion buffer was added and the samples were incubated at 37 °C overnight. Another portion of trypsin (0.3 μg) was added and incubated for an extra 3 h. Peptides were collected by centrifugation and SDC was removed by acidification with 10% trifluoroacetic acid. Samples were further purified using Detergent Removal Spin Column (Pierce, ThermoFischer Scientific) followed by C18 Desalting Spin Column (Pierce, ThermoFischer Scientific) according to the manufacturer's guidelines. The detergent-free supernatants were dried and reconstituted in 3% acetonitrile (ACN) in 0.1% formic acid (FA) for LC-MS analysis.

Peptide samples were analyzed on a QExactive HF mass spectrometer interfaced with Easy-nLC1200 liquid chromatography system (ThermoFisher Scientific). Peptides were trapped on an Acclaim Pepmap 100 C18 trap column (100 μm × 2 cm, particle size 5 μm, ThermoFischer Scientific) and separated on an in-house packed analytical column (75 μm × 300 mm, particle size 3 μm, Reprosil-Pur C18, Dr. Maisch) using a gradient from 9% to 48% B over 75 min, followed by an increase to 100% B for 5 min at a flow of 300 nL/min, where Solvent A was 0.2% FA and solvent B was 80% ACN in 0.2% FA. The instrument

operated in data-dependent mode where the precursor ion mass spectra were acquired at a resolution of 60,000, the 10 most intense ions were isolated in a 1.2 Da isolation window and fragmented using collision energy HCD settings at 28. MS2 spectra were recorded at a resolution of 30,000 with charge states 2 to 4 selected for fragmentation and dynamic exclusion set to 20 s.

Data analysis was performed using Proteome Discoverer version 1.4 (ThermoFisher Scientific) against the *Human* Uniprot Database Nov 2017 (Swiss Institute of Bioinformatics, Switzerland). Mascot 2.5 (Matrix Science) was used as a search engine with precursor mass tolerance of 5 ppm and fragment mass tolerance of 200 millimass units. Tryptic peptides were accepted with one missed cleavage. Variable modification of methionine oxidation and fixed cysteine alkylation were selected. The detected peptide threshold in the software was set to a significance level of Mascot 99% by searching against a reversed database and identified proteins were grouped by sharing the same sequences to minimize redundancy.

2.5. Western Blot Analysis

The proteins were separated with gel electrophoresis, using Novex Bis-Tris 4–12% gels, MES buffer, NuPAGE LDS loading buffer and NuPAGE reducing agent according to the manufacturer's recommendations (ThermoFisher). The proteins were then transferred to a PVDF membrane using a Trans-Blot Turbo system (1.3 A, 25 V for 7 min) and the RTA lf-PVDF kit (Bio-Rad) according to the manufacturer's instructions. Antibody incubations were performed with Super Signal West Femto Rabbit or Mouse kit (ThermoFisher) along with primary antibody incubations overnight: rabbit anti-Atox1 (1 μg/mL, Abcam), mouse anti-GADPH (2 μg/mL, Abcam), mouse anti-cyclin B1 (1 μg/mL, Santa Cruz) or mouse anti-cyclin A (1 μg/mL, Santa Cruz), and detected with ChemiDoc MP (Bio-Rad) using high sensitivity chemiluminescence detection.

2.6. In Situ Proximity Ligation Assay (PLA)

PLA was performed on fixed HEK293T cells using the Duolink® Detection Reagents Green kit (Sigma Aldrich) according to the manufacturer's instructions. Briefly, HEK293T cells were permeabilized in PBS + 0.1% Triton-X-100 for 10 min and washed in PBS. Cells were incubated in blocking solution for 1 h at 37 °C and then with a pair of primary antibodies of different species mouse anti-Atox1 (0.5 μg/mL, Abcam), and rabbit anti-APC1 (1 μg/mL, Novus Biologicals), rabbit anti-APC3 (1 μg/mL, Novus Biologicals), rabbit anti-APC5 (1 μg/mL, Novus Biologicals), rabbit anti-APC7 (1 μg/mL, Novus Biologicals) rabbit anti-beta actin (1 μg/mL, Abcam) or rabbit anti-ATP7A (2 μg/mL, Abcam) overnight at 4 °C. The coverslips were washed in buffer A, followed by incubation with the PLA probes (secondary antibodies against two different species bound to two oligonucleotides: anti-mouse PLUS and anti-rabbit MINUS) for 1 h at 37 °C. Cells were washed in Buffer A and incubated with ligation solution for 30 min, and amplification solution for 100 min, both at 37 °C. The preparations were finally washed in Buffer B, and mounted with Duolink *in situ* mounting medium containing DAPI. Z-stack confocal images were collected through the entire cells at 2 μm interval on an Eclipse Ti 2 inverted microscope (Nikon), equipped with a Nikon 60X/1.4_S oil immersion objective. Maximum intensity projections representing approximately 30% of the cell volume were generated, followed by manual setting of the image threshold at 145–255 to highlight the PLA dots and automatic counting of the PLA dots using the 'Analyze particles' function in Image J software [28]. In order to represent the number of PLA dots per cell, cell numbers were manually counted using the in parallel taken bright field images. Quantification was performed for two independent PLA experiments, whereby all cells were analyzed within 3 to 5 images per condition, with an average cell number per image of 25 (SEM ± 1.17) for HEK293T and 21 (SEM ± 0.90) for HEK293T Atox1 KO. Total cell number analyzed was 187, 232, 206 and 162 for Atox1-APC1, Atox1-APC3, Atox1-APC5 and Atox1-APC7, respectively, in HEK293T cells, and 174, 174, 103 and 143 for Atox1-APC1, Atox1-APC3, Atox1-APC5 and Atox1-APC7, respectively, in HEK293T Atox1 KO cells. Two-sided, unpaired *t*-test was used for statistical analysis.

2.7. Flow Cytometry

Cells were washed with PBS and detached using TrypLE express. The cell pellet was washed with PBS and re-suspended in a small volume of PBS. The cell suspension was added dropwise to ice-cold 99.7% ethanol (Solveco) to a final ethanol concentration of 70% and kept in −20 °C overnight.

Wt and Atox1 KO HEK293T cells were incubated in 10% FBS complete medium for 72 h and were ethanol-fixed before reaching 80% confluency. Cells were then pelleted and resuspended in PBS and added to a round bottom 96-well plate (Nunc) and an equal volume of 2× PI staining solution, containing 1:250 propidium iodide (ThermoFisher) and 1:25 RNase A (ThermoFisher) in PBS, was added. The cells were incubated 2 h at room temperature and 48 h at 4 °C prior to analysis with a Guava EasyCyte 8HT flow cytometer (Merck Millipore).

The red fluorescence of PI was monitored to indirectly examine the DNA content of the cells. Cells were gated using the area versus width plot of the red fluorescence (to exclude doublets), and forward and side scatter. The red fluorescence intensity was analyzed with Guava InCyte software of three technical replicates. The mean cellular fluorescence of three separate experiments was plotted with error bars corresponding to the standard deviation of mean.

2.8. Cell Proliferation Assay

Single cell suspensions were prepared from 80% confluent cell cultures and seeded in 6-well plates (40,000 cells per well). Cells were incubated at 37 °C and 5% CO_2 and cell number was measured using an automatic cell counter (Countess II FL, ThermoFisher Scientific) at 24 h, 48 h and 72 h after cell seeding. We performed three independent experiments, and each individual experiment consisted out of 3 replicas. Live/dead cells were probed after 72 h using a commercial kit (Live/dead viability/cytotoxicity kit, ThermoFisher Scientific). Two-sided, paired *t*-test was used for statistical analysis.

3. Results

3.1. New Atox1 partners identified with co-immunoprecipitation

To find new interaction partners of the Cu chaperone Atox1 in mammalian cells, co-immunoprecipitation (co-IP) experiments were performed in HEK293T cells using antibody-coupled magnetic beads. Because Atox1 is a small (68 residues) protein, extensive optimization was required to obtain successful Atox1 immunoprecipitation from the cell lysate (Fig. 1, Fig. S2). In parallel control experiments, we used an isotype control antibody coupled to the beads. The co-IP samples were analyzed by nano-LC MS/MS for the detection of peptide fragments. A Mascot 99 filter (1% false discovery rate) was used for nano-LC MS/MS analysis and detection of one unique peptide in the Atox1

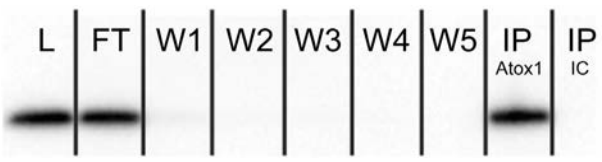

Fig. 1. Western blot detection of Atox1 in co-IP samples: blot. cell lysate (L), flow through (FT), washes (W1–5) and immunoprecipitates (IP) with an Atox1-antibody as bait as well as using an isotype control antibody (IC). See also Fig. S2.

sample but not in the isotype control was regarded a positive result (hit).

Proteins immunoprecipitated with Atox1, but not with the isotype control, and identified with at least four unique peptides in the Atox1 sample, are listed in Table 1. Complete lists of identified proteins (in Atox1 and control samples) in the HEK293T cells are provided in Table S1. Surprisingly, upon inspection of the data in Table 1, it is evident that proteins involved in the cell cycle are the top hits in our experiments. In particular, several anaphase-promoting complex (APC) subunits are found on top of the list of proteins immunoprecipitated with Atox1. The hits with the highest number of unique peptides identified are in descending order APC1, APC7, APC3 and APC5.

Notably, when the same co-IP experiment was performed in the cancer cell line MDA-MB-231, we also found APC subunits (including APC1, APC7, APC3 and APC5 noted above) as the primary proteins immunoprecipitated with Atox1 (overlap in hits between cell lines are marked in Table 1). Complete lists of identified proteins (in Atox1 and control samples) in the MDA-MB-231 cells are reported in Table S2. We note that no known Atox1 partners in the Cu transport chain were immuno-precipitated in our experiments (e.g., Ctr1, ATP7A/B). This observation suggests that this experimental approach favors copper-independent interactions. Therefore, the results obtained here do not necessarily report on *dominant* Atox1 interactions but merely identify APC subunits as being *among* cellular Atox1 interaction partners.

Table 1
Proteins co-immunoprecipitated with Atox1 (using antibody-coupled beads) from HEK293T cells identified by nano-LC MS/MS[a]. Bold gene names indicate subunits of the APC complex'; italic protein description represent proteins (APC subunits and the regulators CDC20 and CDH1) involved in the cell cycle.

Gene name	Protein description	Uniprot Accession	Number of unique peptides
ANAPC1	*Anaphase-promoting complex subunit 1*[b]	Q9H1A4	28
ANAPC7	*Anaphase-promoting complex subunit 7*[b]	Q9UJX3	24
ANAPC3 (CDC27)	*Anaphase-promoting complex subunit*[b]*(Cell division cycle protein 27 homolog)*	P30260	20
ANAPC5	*Anaphase-promoting complex subunit 5*[b]	Q9UJX4	14
ANAPC8 (CDC23)	*Anaphase-promoting complex subunit 8*[b] *(Cell division cycle protein 23 homolog)*	Q9UJX2	13
SARNP	SAP domain-containing ribonucleoprotein[b]	P82979	11
ANAPC2	*Anaphase-promoting complex subunit 2*[b]	Q9UJX6	10
ANAPC6 (CDC16)	*Anaphase Promoting Complex subunit 6*[b]*(Cell division cycle protein 16 homolog)*	Q13042	10
TOMM70	Mitochondrial import receptor subunit TOM70	O94826	10
ANAPC10	*Anaphase-promoting complex subunit 10*[b]	Q9UM13	7
ANAPC4	*Anaphase-promoting complex subunit 4*[b]	Q9UJX5	7
MOGS	Mannosyl-oligosaccharide glucosidase	Q13724	7
LETMD1	LETM1 domain-containing protein 1	Q6P1Q0	6
NEK2	Serine/threonine-protein kinase Nek2	P51955	6
PARP1	Poly [ADP-ribose] polymerase 1	P09874	6
CDC20	*Cell division cycle protein 20 homolog*[b]	Q12834	5
CDH1 (FZR1)	*Fizzy and cell division cycle 20 related 1 (Fizzy-related protein homolog)*	Q9UM11	5
NEK1	Serine/threonine-protein kinase Nek1	Q96PY6	5
ALDH3A2	Fatty aldehyde dehydrogenase	P51648	4
ANAPC16	*Anaphase-promoting complex subunit 16*[b]	Q96DE5	4
C3orf58	Deleted in autism protein 1	Q8NDZ4	4
FAR1	Fatty acyl-CoA reductase	Q8WVX9	4
TMPO	Lamina-associated polypeptide 2, isoforms beta/gamma[b]	P42167	4
SLC25A11	Mitochondrial 2-oxoglutarate/malate carrier protein	Q02978	4
MARC2	Mitochondrial amidoxime reducing component 2	Q969Z3	4
OCIAD1	OCIA domain-containing protein 1	Q9NX40	4
PTGES2	Prostaglandin E synthase 2	Q9H7Z7	4
PHLDB2	Pleckstrin homology-like domain family B member 2	Q86SQ0	4
RPS16	40S ribosomal protein S16[b]	P62249	4
SEC22B	Vesicle-trafficking protein SEC22b	O75396	4
VDAC1	Voltage-dependent anion-selective channel protein 1	P21796	4
XRCC6	X-ray repair cross-complementing protein 6	P12956	4

[a] The list contains proteins identified with at least four unique peptides in the Atox1 co-IP but no peptide in the isotype control co-IP. A complete list of for both Atox1 and isotype control co-IP in the HEK293T cells is found in Table S1.

[b] These proteins were also co-immunoprecipitated with Atox1 in MDA-MB-231 breast cancer cells, see Table S2 for complete list for this cell line.

3.2. Proximity Ligation Assay to Detect Atox1-APC Interactions in Cells

To directly probe Atox1 interactions with APC subunits in the HEK293T cells, we employed the recently developed proximity ligation assay (PLA) which exhibits single-molecule resolution [29,30]. Here, oligonucleotide probes are attached to antibodies against two proteins of interest and, if they are bound in close proximity (< 40 nm), the oligonucleotides guide the formation of circular DNA strands. The DNA circles can then serve as templates for localized rolling-circle amplification which allows pairs of protein molecules in close proximity to be visualized and counted *in situ* using fluorescence microscopy. As a negative control for the PLA experiments, and also used in our other experiments (see below), we created an Atox1 KO cell line of the HEK293T cells (Fig. S1).

We used PLA to assess Atox1 interactions *in situ* for APC1, APC3, APC5 and APC7. The subunits APC1, APC3 and APC7 were selected as they are the top three hits in the immunoprecipitation results in HEK293T cells; APC5 was chosen as it is located further away from APC1, APC3 and APC7 in the structure of the complete APC complex [22,23] but still is among the top four hits in Table 1. Quantitative analysis of the results for Atox1 and APC1, APC3 and APC7, respectively, showed higher number of dots in each case as compared to the background found in the KO cell line (Fig. 2), indicating close proximity between Atox1 and APC1, APC3 and APC7 in the HEK293T cells. However, for APC5, no specific Atox1 interaction was found using PLA, indicating that this APC subunit is not in close proximity of Atox1 and, therefore, likely interacts indirectly with Atox1 via other APC subunits. Notably, the PLA data demonstrates that the interactions between Atox1 and APCs take place in the cytoplasm (Fig. 2). Several control experiments were performed to assess the accuracy of the PLA results. As positive and negative controls we performed PLA for Atox1-ATP7A and Atox1-beta actin interactions, respectively, in wt and Atox1 KO HEK293T cells. We also confirmed the specificity of the anti-Atox1 antibody by a PLA experiment for Atox1 detection using anti-mouse minus and plus PLA probes in wt and Atox1 KO HEK293T cells (Fig. S3). The PLA results, together with the co-IP results, encouraged us to further study a possible role of Atox1 in the cell cycle.

3.3. Consequence for Cells of Atox1 Knock out (KO)

The cell cycle can be divided into interphase (including G_1, S, and G_2 stages) followed by mitosis (M phase, which includes the anaphase) and cytokinesis, with the last two steps facilitating cell division. Anaphase starts when cytoplasmic APC labels an inhibitory chaperone with ubiquitin [22,23] resulting in a cascade of events that promotes sister chromatid separation. Activator subunits target APC to specific sets of substrates at different times in the cell cycle: Cdc20 activates in mitosis and Cdh1 activates in interphase [26]. Atox1 may modulate APC activity at any stage of the cell cycle, as both Cdc20 and Cdh1 were found in the Atox1 co-IP (Table 1).

To probe if Atox1-APC interactions have an effect on cell cycle progression, we first compared the cell cycle distribution of wt and Atox1 KO (Fig. S1) HEK293T cells using flow cytometry. We found that the cell cycle distribution was altered for the KO line: Whereas the wt cells are found to be mostly in G_1 and S phases, the KO cells have an increased population of the G_2/M phases and decreased population of the S phase (Fig. 3, Fig. S4A). Normally, the mammalian cell cycle takes about 20 h, with half of the time being spent in G_1 phase. The G_2/M

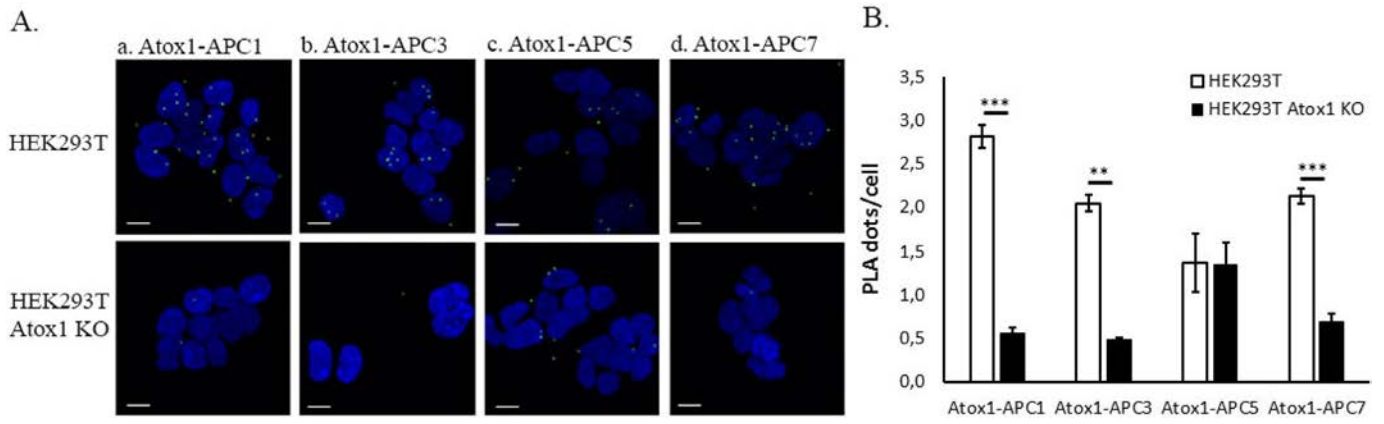

Fig. 2. A. Representative confocal maximum intensity projection images of the *in situ* proximity ligation assay (PLA) between (a) Atox1 and APC1, (b) Atox1 and APC3, (c) Atox1 and APC5, and (d) Atox1 and APC7 in the wt and Atox1 KO HEK293T cells (upper and lower panel, respectively). A positive PLA signal appears as a green dot. Cell nuclei are stained with DAPI (blue color). Scale bars indicate 10 μm. B. Quantitative analysis of the PLA signals using the confocal images in ImageJ software. Results are shown as mean ± SEM. Statistical significance is indicated as follows: *$p < 0.05$, **$p < 0.01$, ***$p < 0.001$ (using the two-sided, unpaired *t*-test). (For interpretation of the references to color in this figure legend, the reader is referred to the web version of this article.)

phases take place during only a few hours and the rest of the time is spent in the S phase. Inspection of the fractions of cells in different phases for the two cell types shows that the fraction of total cell cycle time the cells spend in G_2/M phases has increased from about 23% to 33% when Atox1 is absent (Fig. 3A). As another evidence of altered cell cycle phases, we compared the amounts of cyclins A and B1 in wt and Atox1 KO cells. Both these cyclins are accumulated in G_2/M phases [31] and, in accord with the flow cytometry data, we find a trend of increased cyclins A and B1 in the KO cells (Fig. S4B). Unfortunately, the differences were not statistically significant which may be due to the rather small increase in G_2/M percentage for the KO cells. Taken together, removing Atox1 protein from the cells prolongs the duration of G_2/M phases compared to G_1 and S, resulting in G_2/M enrichment.

That knock out of Atox1 in cells results in slower growth than corresponding wt cells has been reported for mouse embryonic fibroblasts [14]. To link altered cell cycle stage distribution to cell growth of our cells, we probed cell proliferation of wt and Atox1 KO HEK293T cells over 72 h (Fig. 3B). The data shows that the Atox1 KO cells proliferate slower than the wt cells: at 72 h the amount of wt cells is almost double that of the KO cells. To test if the result was due to slower proliferation or increased cell death, we probed the presence of dead cells in both wt and KO cells after 72 h of growth. Data from Live/Dead staining experiments showed that the number of dead cells was low in both cell lines (<2%; data not shown).

Taken together, removal of Atox1 from the cells increases the population of cells in G_2/M phases and slows down overall cell proliferation. A tentative explanation for these observations is that Atox1 is a co-activator of APC, helping it to advance through later stages of the cell cycle, thereby facilitating proliferation.

4. Discussion

We here show that the copper chaperone Atox1, known for transporting Cu in the cytoplasm, interacts with subunits in the anaphase-promoting complex (APC). APC is a 1.2 MDa complex including 19 APC subunits and coactivators that regulates multiple steps in the cell cycle, but most prominently, mitosis [22,23]. High resolution structures of the multi-protein APC complex, with different coactivators bound, have been resolved by cryo-electron microscopy [23,32]. From the deduced arrangement of subunits in the APC complex, the here discovered subunits co-immunoprecipitated with Atox1 can be located to two regions. The top three hits in Table 1 are APC1, APC7 and APC3; these proteins are located near each other on one side of the complex (right side, Fig. 4) and are also closely connected to APC10, APC16 and modulator Cdh1 proteins, also on list in Table 1. The fourth and fifth top hits in Table 1, APC5 and APC8, are located next to each other on the other side of the APC complex (left side, Fig. 4) and are connected to APC2, APC6 and APC4 (also in Table 1). Using *in situ* proximity ligation directly in cells, we confirmed Atox1 interactions (close proximity) for APC1, APC3 and APC7 (top three hits in Table 1) but not for APC5.

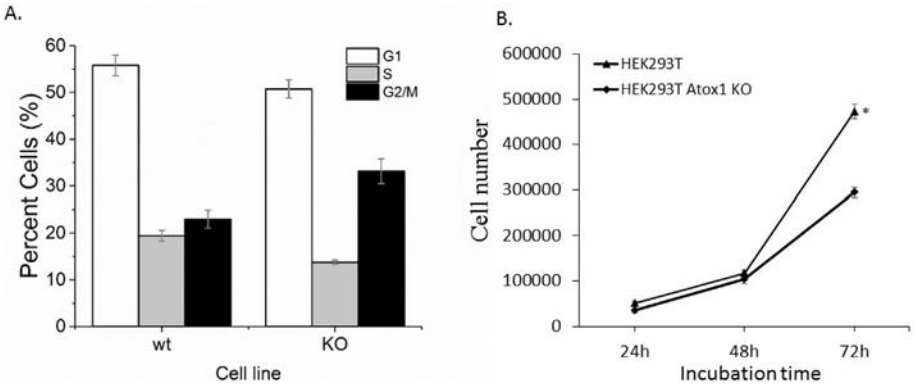

Fig. 3. A. Cell cycle distribution of wt and Atox1 KO HEK293T cells by PI staining and flow cytometry analysis. The percent cells in S phase was decreased ($p < 0.01$) whereas the amount cells with G2/M DNA content was increased for the KO cells ($p < 0.01$). The error bars are standard deviation of mean ($n = 3$). B. Cell proliferation of wt and Atox1 KO HEK293T cells by measurement of total cell number at 24 h, 48 h and 72 h after seeding (40.000 cells/well at time zero). Decreased proliferation rate for Atox1 KO in comparison to wt HEK293T cells. Standard error indicates standard error of the mean, and * indicates $p < 0.001$ with two-sided *t*-test (3 independent experiments with three replicas in each).

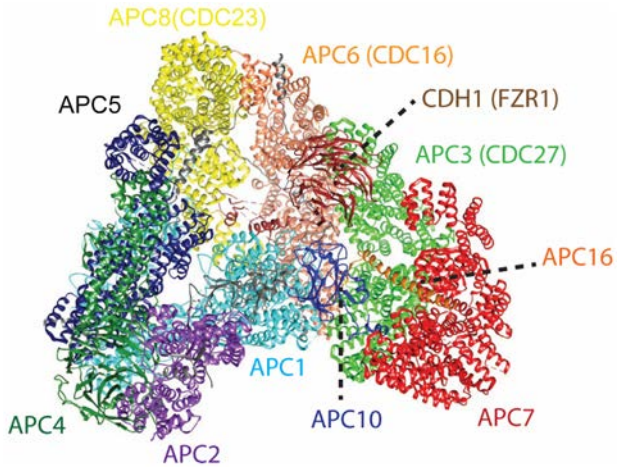

Fig. 4. Structure of anaphase-promoting complex (APC) with the subunits, identified in the co-IP-MS with at least 4 unique peptides, in color. Subunits APC11, APC13, APC15, and F-box only protein 5 were not found in the analysis of the Atox1 co-IP using nano-LC MS/MS and are shown in grey; also in grey is APC12 which was identified in the Atox1 immunoprecipitation experiment with only 2 unique peptides. The subunits identified with largest number of unique peptides are all located in the same area, APC7 (red), APC1 (cyan) and APC3 (light green, also called CDC27). Image made using PDB ID 4UI9 [23] and UCSF Chimera 1.11.2 software [37]. (For interpretation of the references to color in this figure legend, the reader is referred to the web version of this article.)

Therefore, it appears as Atox1 makes interactions in the region occupied by APC1, APC3 and APC7 which, as the APC complex is a stable multi-domain structure, results in co-immunoprecipitation of almost all APC subunits. Thus, APC5 and several other of the APC subunits listed in Table 1 are not interacting directly with Atox1 but are co-immunoprecipitated due to their presence in the APC complex.

Although it remains unclear how/if Atox1 binding affects the activity of the APC complex, we found that removal of Atox1 protein from the HEK293T cells enriches cells in the G_2/M phases and, in parallel, slows down their proliferation rate. Thus, we speculate that Atox1 acts as an activator that upon binding aids APC with progression through later stages of cell division. However, as Atox1 has additional functions in cellular copper metabolism, a direct link between Atox1 interaction with APC and functional effects on the cell cycle and proliferation cannot be made. Additional biochemical and cell biology studies are needed to confirm this idea.

Nonetheless, there are some interesting associations to be noted. In a related study, the global transcriptional response to deletion of the yeast Atox1 homolog gene, Atx1, in *Saccharomyces cerevisiae* was analyzed and the results indicated a possible role of Atx1 in cell cycle related processes in yeast [33]. It was found that several transcripts for proteins related with the meiotic cell cycle and its transcriptional regulation were repressed upon deletion of the Atox1 gene irrespective of the copper level [33]. For mammals, it was proposed that Atox1 was a copper-dependent transcription factor that mediated cell proliferation. It was shown that copper stimulation of mouse embryonic fibroblasts markedly increased cell proliferation, cyclin D1 expression, and entry into S phase; processes which all were completely abolished in Atox1 KO cells [14]. Although there were no biophysical support for Atox1 being a DNA-binding protein directly regulating the cyclin D1 promoter [18], these findings may be interpreted in light of our current results. Cyclin D1 is the main regulator of the cyclin-dependent kinase CDK4 in the G_1 phase and it was shown that, during the metaphase to anaphase transition, APC degrades CDK4 and cyclin D1 is sequestered in the cytoplasm [34]. CDK4 re-accumulates in the following G1 phase and facilitates nuclear import of cyclin D1 [34]; thus without CDK4, cyclin D1 cannot promote S phase. Therefore, we speculate that the reported relationship between Atox1 and Cyclin D1 may involve dysfunction of APC (due to the absence of Atox1) affecting degradation of CDK4 that, in turn, affects cyclin D1 function. Atox1 has also been identified to be important for proliferation of non-small lung cancer cells and it was even proposed that Atox1 may be a potential therapeutic target for lung cancer therapy [35].

The effects of altered copper levels and/or importance of Atox1 being copper-loaded for the here observed cell cycle effects and APC interactions should be specifically addressed in future work. A recent study indicated that small synthetic molecules, blocking the copper-binding ability of Atox1 and of another cytoplasmic copper chaperone, resulted in inhibition of proliferation of cancer cells and these molecules also significantly attenuated tumor growth in xenograft mice models [36]. These effects were proposed to be due to accumulation of free copper ions in cells that caused oxidative damage and killed the cells [36]. Based on our results, part of the noted changes may be due to cell cycle/growth defects due to an abolished Atox1 network of interactions.

In conclusion, we have discovered that the copper chaperone Atox1 interacts with subunits of APC, which is a complex involved in several steps of the cell cycle. Further studies are required to reveal the molecular mechanisms of this interaction and its consequences for the cell cycle. Such studies are of importance as they may reveal new targets for the development of anticancer drugs and, from a fundamental point of view, they may also identify a connection between copper metabolism and the cell cycle.

Role of the Funding Source

The funding sources given above had no role in study design, data collection, analysis and interpretation, or in writing and submission of the report.

Acknowledgements

The proteomic analysis was performed at the Proteomics Core Facility of Sahlgrenska Academy, University of Gothenburg. Molecular graphics were performed with the UCSF Chimera package. The Nikon confocal microscope was funded by the Lundberg foundation, Sweden. Funding for research was provided by the Swedish Research Council, the Knut and Alice Wallenberg Foundation and the Swedish Cancer Society.

Appendix A. Supplementary data

Supplementary data to this article can be found online at https://doi.org/10.1016/j.csbj.2018.10.018.

References

[1] Huffman DL, O'Halloran TV. Function, structure, and mechanism of intracellular copper trafficking proteins. Annu Rev Biochem 2001;70:677–701.
[2] Puig S, Thiele DJ. Molecular mechanisms of copper uptake and distribution. Curr Opin Chem Biol 2002;6:171–80.
[3] Harris ED. Basic and clinical aspects of copper. Crit Rev Clin Lab Sci 2003;40:547–86.
[4] Valko M, Morris H, Cronin MT. Metals, toxicity and oxidative stress. Curr Med Chem 2005;12:1161–208.
[5] O'Halloran TV, Culotta VC. Metallochaperones, an intracellular shuttle service for metal ions. J Biol Chem 2000;275:25057–60.
[6] Festa, R. A., and D. J. Thiele. Copper: an essential metal in biology. Curr Biol 21:R877–883.
[7] Robinson NJ, Winge DR. Copper metallochaperones. Annu Rev Biochem 2010;79:537–62.
[8] Ohrvik H, Thiele DJ. How copper traverses cellular membranes through the mammalian copper transporter 1, Ctr1. Ann N Y Acad Sci 2014;1314:32–41.
[9] Ariöz C, Wittung-Stafshede P. Folding of copper proteins: role of the metal? Q Rev Biophys 2018;51:e4.
[10] Arioz C, Li Y, Wittung-Stafshede P. The six metal binding domains in human copper transporter, ATP7B: molecular biophysics and disease-causing mutations. Biometals 2017;30:823–40.
[11] Wittung-Stafshede P. Unresolved questions in human copper pump mechanisms. Q Rev Biophys 2015;48:471–8.
[12] Lutsenko S, Leshane ES, Shinde U. Biochemical basis of regulation of human copper-transporting ATPases. Arch Biochem Biophys 2007;463:134–48.
[13] Yamamoto T, Ebisuya M, Ashida F, Okamoto K, Yonehara S, Nishida E. Continuous ERK activation downregulates antiproliferative genes throughout G1 phase to allow cell-cycle progression. Curr Biol 2006;16:1171–82.

[14] Itoh S, Kim HW, Nakagawa O, Ozumi K, Lessner SM, Aoki H, et al. Novel role of antioxidant-1 (Atox1) as a copper-dependent transcription factor involved in cell proliferation. J Biol Chem 2008;283:9157–67.
[15] Itoh S, Ozumi K, Kim HW, Nakagawa O, McKinney RD, Folz RJ, et al. Novel mechanism for regulation of extracellular SOD transcription and activity by copper: role of antioxidant-1. Free Radic Biol Med 2009;46:95–104.
[16] Ozumi K, Sudhahar V, Kim HW, Chen GF, Kohno T, Finney L, et al. Role of copper transport protein antioxidant 1 in angiotensin II-induced hypertension: a key regulator of extracellular superoxide dismutase. Hypertension 2012;60:476–86.
[17] Chen GF, Sudhahar V, Youn SW, Das A, Cho J, Kamiya T, et al. Copper transport protein antioxidant-1 promotes inflammatory neovascularization via chaperone and transcription factor function. Sci Rep 2015;5:14780.
[18] Kahra D, Mondol T, Niemiec MS, Wittung-Stafshede P. Human copper chaperone Atox1 translocates to the nucleus but does not bind DNA in vitro. Protein Pept Lett 2015;22:532–8.
[19] Ohrvik H, Wittung-Stafshede P. Identification of new potential interaction partners for human cytoplasmic copper chaperone Atox1: roles in gene regulation? Int J Mol Sci 2015;16:16728–39.
[20] Blockhuys S, Wittung-Stafshede P. Copper chaperone Atox1 plays role in breast cancer cell migration. Biochem Biophys Res Commun 2017;483:301–4.
[21] Matson Dzebo M, Arioz C, Wittung-Stafshede P. Extended functional repertoire for human copper chaperones. Biomol Concepts 2016;7:29–39.
[22] Alfieri C, Zhang S, Barford D. Visualizing the complex functions and mechanisms of the anaphase promoting complex/cyclosome (APC/C). Open Biol 2017;7.
[23] Chang LF, Zhang Z, Yang J, McLaughlin SH, Barford D. Molecular architecture and mechanism of the anaphase-promoting complex. Nature 2014;513:388–93.
[24] Chang L, Barford D. Insights into the anaphase-promoting complex: a molecular machine that regulates mitosis. Curr Opin Struct Biol 2014;29:1–9.
[25] Peters J-M. The anaphase-promoting complex: proteolysis in mitosis and beyond. Mol Cell 2002;9:931–43.
[26] Castro A, Bernis C, Vigneron S, Labbé J-C, Lorca T. The anaphase-promoting complex: a key factor in the regulation of cell cycle. Oncogene 2005;24:314.
[27] Wiśniewski JR, Zougman A, Nagaraj N, Mann M. Universal sample preparation method for proteome analysis. Nat Methods 2009;6:359.
[28] Gomes I, Sierra S, Devi LA. Detection of receptor heteromerization using in situ proximity ligation assay. Curr Protoc Pharmacol 2016;75:31 2 16 11-12 16.
[29] Fredriksson S, Gullberg M, Jarvius J, Olsson C, Pietras K, Gústafsdóttir SM, et al. Protein detection using proximity-dependent DNA ligation assays. Nat Biotechnol 2002;20:473.
[30] Söderberg O, Gullberg M, Jarvius M, Ridderstråle K, Leuchowius K-J, Jarvius J, et al. Direct observation of individual endogenous protein complexes in situ by proximity ligation. Nat Methods 2006;3:995.
[31] Jackman MR, Pines JN. Cyclins and the G2/M transition. Cancer Surv 1997;29:47–73.
[32] Chang L, Zhang Z, Yang J, McLaughlin SH, Barford D. Atomic structure of the APC/C and its mechanism of protein ubiquitination. Nature 2015;522:450.
[33] Cankorur-Cetinkaya A, Eraslan S, Kirdar B. Transcriptomic response of yeast cells to ATX1 deletion under different copper levels. BMC Genomics 2016;17:489.
[34] Chen H, Xu X, Wang G, Zhang B, Wang G, Xin G, et al. CDK4 is degraded by APC/C in mitosis and reaccumulates in early G1 phase to initiate a new cell cycle in HeLa cells. J Biol Chem 2017;292:10131–41.
[35] Cai H, Peng F. Knockdown of copper chaperone antioxidant-1 by RNA interference inhibits copper-stimulated proliferation of non-small cell lung carcinoma cells. Oncol Rep 2013;30:269–75.
[36] Wang J, Luo C, Shan C, You Q, Lu J, Elf S, et al. Inhibition of human copper trafficking by a small molecule significantly attenuates cancer cell proliferation. Nat Chem 2015;7:968–79.
[37] Pettersen EF, Goddard TD, Huang CC, Couch GS, Greenblatt DM, Meng EC, et al. UCSF Chimera—a visualization system for exploratory research and analysis. J Comput Chem 2004;25:1605–12.